HHS Public Access

Author manuscript

Conf Proc (Midwest Symp Circuits Syst). Author manuscript; available in PMC 2016 August 01.

Published in final edited form as:

Conf Proc (Midwest Symp Circuits Syst). 2015 August ; 2015: .

Surface-Based Morphometric Analysis of Hippocampal Subfields in Mild Cognitive Impairment and Alzheimer's Disease

Shan Cong,
Dept. of Electrical and Computer Engineering, Purdue University Indianapolis, Indianapolis, IN 46202

Maher Rizkalla,
Dept. of Electrical and Computer Engineering, Purdue University Indianapolis, Indianapolis, IN 46202

Paul Salama,
Dept. of Electrical and Computer Engineering, Purdue University Indianapolis, Indianapolis, IN 46202

John West,
Dept. of Radiology and Imaging Sciences, Indiana University School of Medicine, Indianapolis, IN 46202

Shannon Risacher,
Dept. of Radiology and Imaging Sciences, Indiana University School of Medicine, Indianapolis, IN 46202

Andrew Saykin, and
Dept. of Radiology and Imaging Sciences, Indiana University School of Medicine, Indianapolis, IN 46202

Li Shen[†] on behalf of ADNI
Dept. of Radiology and Imaging Sciences, Indiana University School of Medicine, Indianapolis, IN 46202

Shan Cong: scong@iupui.edu; Maher Rizkalla: mrizkall@iupui.edu; Paul Salama: psalamag@iupui.edu; John West: jdwest@iupui.edu; Shannon Risacher: srisache@iupui.edu; Andrew Saykin: asayking@iupui.edu; Li Shen: shenli@iu.edu

Abstract

The hippocampus is widely studied with neuroimaging techniques given its importance in learning and memory and its potential as a biomarker for Alzheimer's disease (AD). Its complex folding anatomy often presents analytical challenges. In particular, the critical subfield information is typically not addressed by the existing hippocampal shape studies. To bridge this gap, we present a computational framework for surface-based morphometric analysis of hippocampal subfields. The major strengths of this framework are as follows: (a) it performs detailed hippocampal shape analysis, (b) it embraces, rather than ignores, the important hippocampal subfield information, and

[†]Data used in preparation of this article were obtained from the Alzheimer's Disease Neuroimaging Initiative (ADNI) database (adni.loni.usc.edu). As such, the investigators within the ADNI contributed to the design and implementation of ADNI and/or provided data but did not participate in analysis or writing of this report. A complete listing of ADNI investigators can be found at: http://adni.loni.usc.edu/wpcontent/uploads/how_to_apply/ADNI_Acknowledgement_List.pdf.

(c) it analyzes regular magnetic resonance imaging scans and is applicable to large scale studies. We demonstrate its effectiveness by applying it to the identification of regional hippocampal subfield atrophy patterns associated with mild cognitive impairment and AD.

I. INTRODUCTION

Alzheimer's disease (AD) is a neurodegenerative disorder characterized by progressive impairment of memory and other cognitive functions. The hippocampus is known to play important roles in consolidating information from short-term memory to long-term memory and is one of the first regions of the brain to suffer damage in the progression of AD. Hippocampal measures extracted from magnetic resonance imaging (MRI) scans have been widely studied to detect the status of AD or mild cognitive impairment (MCI, a prodromal stage of AD) [1]–[4] or infer cognitive status [5]. These hippocampal measures include: (a) total volumes [2], [3], (b) subfield volumes [1], [4], (c) surface deformations [5] using surface-based morphometry (SBM), and (d) gray matter (GM) measures using voxel-based morphometry (VBM) [3].

The first two types of measures are highly summarized size measures and may not be able to capture detailed regional changes. The second two types are detailed measures of hippocampal morphometry and have the potential to localize the structural changes in hippocampus. The hippocampus is composed of multiple subfields [6], and the neuron loss is not uniformly distributed on the whole hippocampus [7]. Many hippocampal studies have indicated that subfields play an important role in brain functions, e.g., cornu ammonis 1 (CA1) related to autobiographical memory retrieval [8], CA3 and dentate gyrus (DG) involved in memory encoding and early retrieval [6], and subiculum and CA1 predominantly affected for AD patients [9]. However, this critical subfield information is typically not addressed by the existing SBM and VBM studies [3], [5]. To bridge this gap, we propose a SBM framework that maps hippocampal regional changes onto it subfields and demonstrate its effectiveness by applying it to identifying regional subfield changes in MCI and AD.

The complex folding anatomy of hippocampus presents analytical challenges, and the hippocampal subfield information is often difficult to extract. Most existing subfield studies employed manual segmentation [10]–[12] or semi-automated segmentation [1], [13], coupled with high-field MR technologies (e.g., 4–9.4T) and/or postmortem samples. They often require long scan time and thus is not applicable to large-scale studies. Among very few tools available for hippocampal subfield studies, FreeSurfer (http://freesurfer.net/) recently released a promising routine (http://freesurfer.net/fswiki/HippocampalSubfieldSegmentation) for subfield segmentation [14]. But FreeSurfer tends to yield noisy boundary of the entire hippocampus, which is not suitable for detailed shape analysis [2], [15]. FIRST (http://www.fmrib.ox.ac.uk/fsl/fsl/list.html) [16], an integrated surface registration and segmentation tool developed as part of the FMRIB Software Library (FSL), has produced satisfactory segmentation results of the entire hippocampus for detailed shape studies (e.g., [17], [18]); but it does not offer capability for segmenting subfields. Cong et al. [15] integrated the subfield segmentation results from FreeSurfer, the hippocampal segmentation results from FIRST, and a powerful spherical harmonics

(SPHARM) shape modeling method [19], [20], and developed an approach to build a surface atlas of hippocampal subfields from MRI scans.

In this paper, we propose a novel SBM framework for identifying hippocampal subfield changes related to a certain condition of interest (e.g., age, gender, or diagnosis). We employ the method by Cong et al. [15] to create a surface atlas of hippocampal subfields, use the SPHARM technique to register each individual hippocampus to this atlas, and perform statistical shape analysis on the surface manifold using random field theory [21], [22]. The major strengths of this framework are as follows: (a) it performs detailed hippocampal shape analysis, (b) it embraces, rather than ignores, the important hippocampal subfield information, and (c) it analyzes regular MRI scans and is applicable to large scale studies. We demonstrate its effectiveness via an application to the Alzheimer's Disease Neuroimaging Initiative (ADNI) data set [23].

II. MATERIALS AND METHODS

We follow the three-step pipeline described in [15]: (a) automatic segmentation of the hippocampus (by FIRST) and subfields (by FreeSurfer), (b) modeling hippocampal surfaces using SPHARM, and (c) creating surface atlas of hippocampal subfields. We apply this pipeline and create a surface atlas of hippocampal subfields using all healthy control (HC) participants in the analyzed ADNI data. After that, we register all the individual hippocampal surface to this atlas, and extract surface signals. Finally, we perform statistical shape analysis of these surface signals using random field theory to identify hippocampal subfield regions related to conditions of interest including age, gender, and diagnosis.

A. Test Data

The data used in this study were downloaded from the ADNI database [23]. One goal of ADNI has been to test whether serial MRI, positron emission tomography, other biological markers, and clinical and neuropsychological assessment can be combined to measure the progression of MCI and early AD. For up-to-date information, see www.adni-info.org. We downloaded baseline 3T MRI scans of 172 HC, 267 early MCI (EMCI), 140 late MCI (LMCI), and 108 AD participants aging between 55 and 90, along with demographic and diagnostic information. All the raw data are 3D T1-weighted scans with $1.2 \times 1.0 \times 1.0\ mm^3$ voxel resolution, and dimension of $196 \times 256 \times 256$.

B. Hippocampal Surface Modeling

Automatic hippocampal segmentation is conducted by FIRST. Topology fix is performed on the binary segmentation results to make sure that each hippocampal surface has spherical topology. The SPHARM method is used to model each surface as follows: (a) Spherical parametrization is first performed to establish a bijective mapping between each surface location $v = (x; y; z)^T$ and a pair of spherical coordinates (θ, φ) while minimizing area distortion. This mapping can be represented as: $v(\theta, \varphi) = (x(\theta, \varphi); y(\theta, \varphi); z(\theta, \varphi))^T$. (b) Each parameterized surface is then expanded using spherical harmonics (i.e., Fourier basis functions on the sphere):

$$v(\theta,\phi)=\sum_{l=0}^{\infty}\sum_{m=-l}^{l} c_l^m Y_l^m$$

where Y_l^m is the spherical harmonic of degree *l* and *m*, and coefficients $c_l^m=\left(c_{xl}^m, c_{yl}^m, c_{zl}^m\right)^T$ can be calculated up to a user-desired degree, and estimated by solving a set of linear equations in a least squares fashion [24]. (c) After that, the hippocampal surface can be reconstructed with these estimated coefficients. Using more coefficients leads to a more detailed reconstruction. (d) These SPHARM surfaces can be registered together by aligning their first order ellipsoids (FOEs) (see [15] for details).

C. Hippocampal Subfield Mapping and Atlas Construction

FreeSurfer is used to segment out 8 hippocampal subfields: hippocampal tail, CA1, CA2-3, CA4-DG, fimbria, hippocampal fissure, presubiculum, and subiculum. Since the subfield segmentation process is based on a Bayesian model, each subfield segmentation result is represented as a probability map. We employ the SPHARM basis functions to expand these probability maps, using the same spherical parameterization described above. As a result, for each subfield and each surface location, there is an associated probability value. By comparing the reconstructed probability values from each subfield, each surface location can be labeled by the subfield with the largest probability value.

To facilitate comparison among hippocampal surfaces, we use all the HC data and create a surface atlas to represent an average normal hippocampus. Our method is as follows: (1) let the atlas be the first surface; (2) register each surface to the atlas by aligning their FOEs; (3) let the atlas be the mean of all the data; (4) repeat (2) and (3) until the atlas converges. Each atlas surface location is labeled by the most popular subfield carried by the HC participants. As a result, no atlas surface location is labeled by fimbria and hippocampal fissure. Following a general delineation in [25], we also combine presubiculum and subiculum into one joint subfield denoted as SUB. Consequently, we have five hippocampal subfields shown on the atlas surface in this study (see Figure 1), which is in accordance with prior studies [4], [10], [11], [26].

D. Statistical Shape Analysis on the Surface

We use x_t to denote the atlas, and x to denote an individual surface registered to the atlas. Although the deformation field $\delta(x) = x - x_t$ can be used to describe the individual shape, there are three related elements (corresponding to *x*, *y*, *z* coordinates) in $\delta(x)$ that are needed to capture local shape changes. For simplicity, we look at only the deformation signal along the surface normal direction to reduce the number of variables considered for each surface location. We apply heat kernel smoothing, which generalizes Gaussian kernel smoothing to arbitrary Riemannian manifolds [27], to smooth the surface signals and increase the signal-to-noise ratio. We use a kernel size of 5mm full-width-half-max (FWHM) in the smoothing.

We perform statistical surface analysis to detect: (a) age or gender effect on surface deformation, and (b) group difference (HC vs EMCI, HC vs LMCI, and HC vs AD) on

surface deformation after removing the age and gender effects. We consider the following general linear model (GLM):

$$y = X\Psi + Z\Phi + \epsilon \quad (1)$$

where the dependent variable y is our surface signal; $X = (x_1,\cdots,x_p)$ are the variables of interest such as Group; $Z = (z_1,\cdots,z_k)$ are the variables whose effects we want to exclude, such as Age and Gender; and $\Psi = (\psi_1,\cdots,\psi_k)^T$, $\Phi = (\varphi_1,\cdots,\varphi_p)^T$ and ϵ are the coefficients. The goal is to test if X is significant (i.e., $= \Psi \neq 0$) for some $y \in \partial\Omega$, where $\partial\Omega$ indicates the atlas surface manifold. We use SurfStat [22] to test our GLMs. SurfStat is a Matlab toolbox for the statistical analysis of univariate and multivariate surface and volumetric data using linear mixed effects models and random field theory (RFT, for multiple comparison correction) [28].

III. EXPERIMENTAL RESULTS

Shown in Figure 1 is the resulting surface atlas color-mapped with five hippocampal subfields. Shown in Figure 2 are example T-maps (maps of t statistics) and P-maps (maps of p values, only significant p-values shown, corrected by RFT at both vertex and cluster levels) of selected analyses. Shown in Table I are the numbers of significant surface vertices in each of five analyses.

Below we briefly review the results of three diagnostic effects (covaried for age and gender) on surface signals. (1) HC vs EMCI: There was no significant shape change on the entire surface. (2) HC vs LMCI: LMCI demonstrated significant atrophy patterns in 25% of tail, 38% of CA1, 30% of CA2-3, 32% of CA4-DG, and 55% of SUB. (3) HC vs AD: AD demonstrated significant atrophy patterns in 49% of tail, 87% of CA1, 50% of CA2-3, 94% of CA4-DG, and 84% of SUB. While SUB was among the top atrophy regions at both LMCI and AD stages, CA1 and CA4-DG showed modest atrophy at the LMCI stage but severe atrophy at the AD stage.

Regarding the age, it affected 83% of SUB, 50–56% of Tail, CA1 and CA2-3, and 39% of CA4-DG. The overall pattern was similar to diagnostic effects of LMCI and AD. As to the gender, it affected 47–62% of Tail and CA1, 14–16% of CA2-3 and SUB, and 5% of CA4-DG.

IV. CONCLUSIONS AND DISCUSSIONS

A computational framework has been presented for surface-based morphometric analysis of hippocampal subfields. The major strengths of this framework are as follows: (a) it performs detailed hippocampal shape analysis, (b) it embraces, rather than ignores, the important hippocampal subfield information, and (c) it analyzes regular MRI scans and is applicable to large scale studies. We have demonstrated its effectiveness by applying it to the ADNI data. After controlling the effects of age and gender, we have identified that pre-subiculum and subiculum were among top atrophy regions at both LMCI and AD stages, and CA1 and CA4-DG showed modest atrophy at the LMCI stage but severe atrophy at the AD stage. In this initial effort, we have embraced and mapped the sub-field information in hippocampal

morphometric analyses. One future direction is to use this important subfield information to guide hippocampal surface registration and facilitate more accurate and robust modeling and analysis of the hippocampal 3D structure.

Acknowledgments

This work was supported by IUPUI RSFG, NSF IIS-1117335, DOD W81XWH-14-2-0151, NCAA 14132004, NIH R01 LM011360, U01 AG024904, P30 AG10133, R01 AG042437, and UL1 TR001108. Data collection and sharing for this project was funded by the Alzheimer's Disease Neuroimaging Initiative (ADNI) (National Institutes of Health Grant U01 AG024904) and DOD ADNI (Department of Defense award number W81XWH-12-2-0012). ADNI is funded by the National Institute on Aging, the National Institute of Biomedical Imaging and Bioengineering, and through generous contributions from many other sources. Detailed Acknowledgements information is available in http://adni.loni.usc.edu/wp-content/uploads/how_to_apply/ADNI_Manuscript_Citations.pdf.

References

1. Pluta J, Yushkevich P, et al. In vivo analysis of hippocampal subfield atrophy in mild cognitive impairment via semi-automatic segmentation of T2-weighted MRI. Journal of Alzheimer's Disease. 2012; 31(1):85–99.
2. Shen L, Saykin AJ, et al. Comparison of manual and automated determination of hippocampal volumes in MCI and early AD. Brain imaging and behavior. 2010; 4(1):86–95. [PubMed: 20454594]
3. Testa C, Laakso MP, et al. A comparison between the accuracy of voxel-based morphometry and hippocampal volumetry in Alzheimer's disease. J Magn Reson Imaging. 2004; 19(3):274–82. [PubMed: 14994294]
4. Yushkevich PA, Pluta JB, et al. Automated volumetry and regional thickness analysis of hippocampal subfields and medial temporal cortical structures in mild cognitive impairment. Human brain mapping. 2015; 36(1):258–287. [PubMed: 25181316]
5. Lim HK, Hong SC, et al. Hippocampal shape and cognitive performance in amnestic mild cognitive impairment. Neuroreport. 2012; 23(6):364–8. [PubMed: 22336874]
6. Mueller SG, Chao L, et al. Evidence for functional specialization of hippocampal subfields detected by MR subfield volumetry on high resolution images at 4t. Neuroimage. 2011; 56(3):851–857. [PubMed: 21419225]
7. West MJ, Kawas CH, et al. Hippocampal neurons in pre-clinical Alzheimers disease. Neurobiology of aging. 2004; 25(9):1205–1212. [PubMed: 15312966]
8. Bartsch T, Döhring J, et al. CA1 neurons in the human hippocampus are critical for autobiographical memory, mental time travel, and autonoetic consciousness. Proceedings of the National Academy of Sciences. 2011; 108(42):17562–17567.
9. Rössler M, Zarski R, et al. Stage-dependent and sector-specific neuronal loss in hippocampus during Alzheimer's disease. Acta neuropathologica. 2002; 103(4):363–369. [PubMed: 11904756]
10. Winterburn JL, Pruessner JC, et al. A novel in vivo atlas of human hippocampal subfields using high-resolution 3T magnetic resonance imaging. Neuroimage. 2013; 74:254–265. [PubMed: 23415948]
11. Wisse L, Gerritsen L, Zwanenburg JJ, et al. Subfields of the hippocampal formation at 7T MRI: In vivo volumetric assessment. Neuroimage. 2012; 61(4):1043–1049. [PubMed: 22440643]
12. Joie RL, Fouquet M, et al. Differential effect of age on hippocampal subfields assessed using a new high-resolution 3T MR sequence. NeuroImage. 2010; 53(2):506–514. [PubMed: 20600996]
13. Hunsaker MR, Amaral DG. A semi-automated pipeline for the segmentation of rhesus macaque hippocampus: Validation across a wide age range. PloS one. 2014; 9(2):e89456. [PubMed: 24586791]
14. Van Leemput K, Bakkour A, et al. Automated segmentation of hippocampal subfields from ultra-high resolution in vivo MRI. Hippocampus. 2009; 19(6):549–557. [PubMed: 19405131]

15. Cong S, Rizkalla M, et al. Building a surface atlas of hippocampal subfields from MRI scans using FreeSurfer, FIRST and SPHARM. Circuits and Systems (MWSCAS), 2014 IEEE 57th International Midwest Symposium on. IEEE. 2014:813–816.
16. Patenaude B, Smith SM, et al. A Bayesian model of shape and appearance for subcortical brain segmentation. Neuroimage. 2011; 56(3):907–922. [PubMed: 21352927]
17. Luders E, Thompson PM, et al. Global and regional alterations of hippocampal anatomy in long-term meditation practitioners. Hum Brain Mapp. 2013; 34(12):3369–75. [PubMed: 22815233]
18. Shi J, Thompson PM, et al. Surface fluid registration of conformal representation: application to detect disease burden and genetic influence on hippocampus. Neuroimage. 2013; 78:111–34. [PubMed: 23587689]
19. Shen L, Farid H, McPeek MA. Modeling three-dimensional morphological structures using spherical harmonics. Evolution. 2009; 63(4):1003–1016. [PubMed: 19154365]
20. Shen L, Kim S, et al. Fourier methods for 3D surface modeling and analysis. Emerging Topics in Computer Vision and Its Applications. 2012; 1:175.
21. Worsley K, Marrett S, et al. A unified statistical approach for determining significant signals in images of cerebral activation. Human Brain Mapping. 1996; 4:58–73. [PubMed: 20408186]
22. Worsley, KJ. SurfStat. http://www.math.mcgill.ca/keith/surfstat
23. Weiner MW, Veitch DP, et al. The Alzheimer's Disease Neuroimaging Initiative: a review of papers published since its inception. Alzheimers Dement. 2013; 9(5):e111–94. [PubMed: 23932184]
24. Shen L, Chung MK. Large-scale modeling of parametric surfaces using spherical harmonics. 3D Data Processing, Visualization, and Transmission, Third International Symposium on. IEEE. 2006:294–301.
25. Adler DH, Pluta J, et al. Histology-derived volumetric annotation of the human hippocampal subfields in postmortem MRI. Neuroimage. 2014; 84:505–523. [PubMed: 24036353]
26. Henry TR, Chupin M, et al. Hippocampal sclerosis in temporal lobe epilepsy: findings at 7 t. Radiology. 2011; 261(1):199–209. [PubMed: 21746814]
27. Chung MK, Robbins S, et al. Cortical thickness analysis in autism via heat kernel smoothing. NeuroImage. 2005; 25:1256–1265. [PubMed: 15850743]
28. Worsley KJ, Andermann M, Koulis M, et al. Detecting changes in non-isotropic images. Human Brain Mapping. 1999; 8:98–101. [PubMed: 10524599]

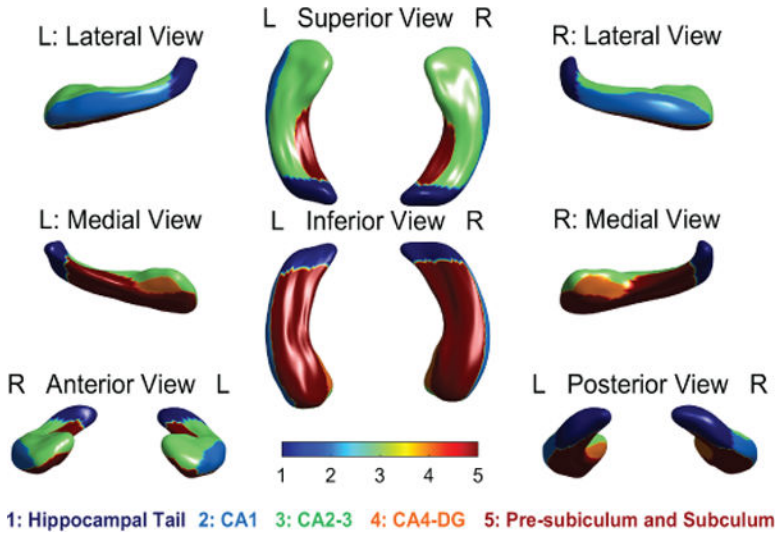

Fig. 1.

Hippocampal surface atlas: five subfields color mapped on to the mean hippocampal surface of all HC participants in the studied cohort.

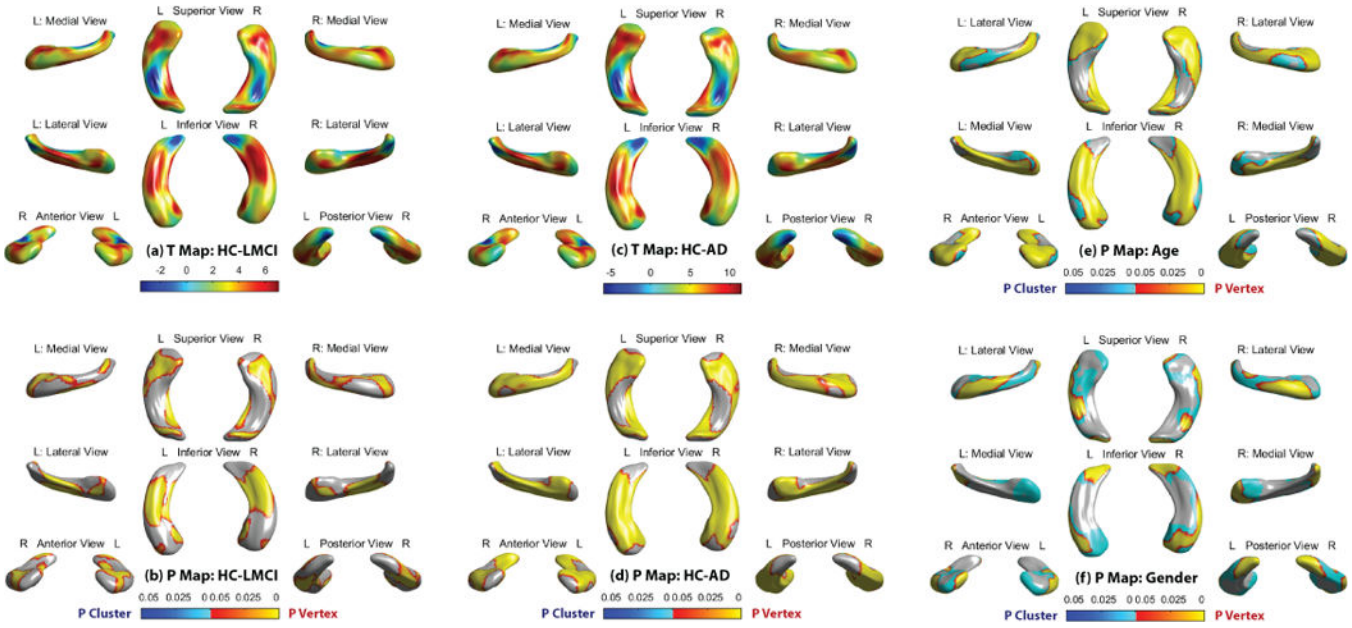

Fig. 2.

(a–b) The t-map and p-map of the diagnostic effect (HC-LMCI) on surface signals after removing the effects of age and gender. (c–d) The t-map and p-map of the diagnostic effect (HC-AD) on surface signals after removing the effects of age and gender. (e) The p-map of age effect on surface signals. (f) The p-map of gender effect on surface signals. In t maps (a,c), red/blue colors respectively indicate expansion/contraction in HC compared with LMCI or AD.

TABLE I

The number of significant surface vertices in each subfield for five different analyses. SUB = pre-subicumlum and subiculum.

Hemisphere		**Left**					**Right**				
Subfields		**Tail**	**CA1**	**CA2-3**	**CA4-DG**	**SUB**	**Tail**	**CA1**	**CA2-3**	**CA4-DG**	**SUB**
Number of vertices		398	389	728	91	956	405	362	735	119	941
Significant Region (number of vertices)	HC vs EMCI	0	0	0	0	0	0	0	0	0	0
	HC vs LMCI	89	135	236	33	550	112	151	210	35	494
	HC vs AD	201	343	365	88	837	193	307	365	110	762
	Age	223	195	346	52	803	201	225	389	29	766
	Gender	181	235	111	0	81	196	231	120	10	184

Conf Proc (Midwest Symp Circuits Syst). Author manuscript; available in PMC 2016 August 01.